Optimization of Transmitter Semi-Angle and Ambient Noise Cancellation for Indoor Visible Light Communications

Aanchal Verma[1,*] and Amritanshu Pandey[1]

ARTICLEINFO

Article history:
Received: 16 June 2021
Revised: 31 August 2021
Accepted: 25 November 2021

Keywords:
LED semi-angle
Visible light communication
LOS channel model
Differential receiver
Ambient noise

ABSTRACT

Visible light communication (VLC) is unquestionably a viable method for dealing with the ever-increasing traffic on wireless networks. Light-emitting diodes (LEDs), which are used for lighting, can be used to convey high-speed data. The optical power determines the indoor VLC link performance. A fundamental challenge in this regard is to design an optimized design of visible light communication with the uniform power distribution and minimize the interference of the ambient light in the daytime. The optimization of transmitter semi-angle and ambient noise cancellation for indoor visible light communications is discussed in this study. The study shows that lowering the semi-angle improves average received optical power while raising power fluctuations on the receiver's plane. In order to resolve this trade-off, we use a unique and simple optimization method for calculating the appropriate transmitter semi-angle that maximizes received power while reducing power variation around the room. By adjusting the number of LED panels and their placements on the plane of the transmitter, the best configuration based on the optimization function is selected. The effects of utilizing a differential optical receiver on SNR distribution in optimal VLC indoor configuration is discussed, which results in better SNR, and the ability to suppress ambient light and other atmospheric noise.

1. INTRODUCTION

Due to the tremendous rise in internet traffic over the past two decades, new communication technologies that take advantage of previously unexplored parts of the electromagnetic spectrum are urgently needed. Many research in the field of wireless optical communication [15], notably visible light communication (VLC) transfers data using a white light-emitting diodes (LEDs) [1–3], are being done for this purpose. Due to improvements in the area of solid-state lighting technologies [12]-[14], VLC has received a lot of attention [4]. Aside from that, it has a number of other advantages, such as less electromagnetic interference, unlicensed spectrum, radiation safety, and increased security against spying [1–4].

White light LEDs will soon entirely dominate interior illumination; hence VLC research is currently focused on indoor infrastructure to device communication. Instead of having a uniform distribution of transmitters illumination, practical LED illumination systems are arranged as panels of many LEDs that focus transmitters in specific sections of the room. The optical power on the receiver's plane is thus uneven or bumpy as a result, degrading the performance of indoor VLC networks significantly [7]-[9]. The power distribution is primarily determined by two factors: the semi-angle of the transmitter and the design of many transmitters. Furthermore, due to the Lambertian order of the radiation pattern, the semi-angle of LEDs is finite.

The semi-angle of LED transmitters has a significant impact on the spatial distribution of optical power received. Increased LED semi-angle lowers spatial fluctuations while simultaneously increasing losses, resulting in a decrease in average power received. This trade-off situation needs a method for determining the best value of semi-angle, the author of [5], described a method for optimization. The power distribution is primarily determined by two factors: the semi-angle of the transmitter and the design of many transmitters.

We will use the unique optimization strategy of [5] for reducing non-uniformity without sacrificing average received power, resulting in an optimal LED semi-angle value in a relatively larger dimension. Second, we will investigate the optimized configuration between 4(2x2) to 81(9x9) number of panels. Third, after optimization of the semi-angle, we will reduce ambient noise by using a differential optical filter at the receiver side, which will increase SNR.

[1]*Department of Electronics Engineering, Indian Institute of Technology (Banaras Hindu University) Varanasi, U.P., (221005), India.*
**Corresponding author:* Aanchal Verma; Phone: +91-7974835674; E-mail: aanchalverma.ece19@iitbhu.ac.in.

2. SYSTEM MODEL

2.1 Light propagation and received optical power

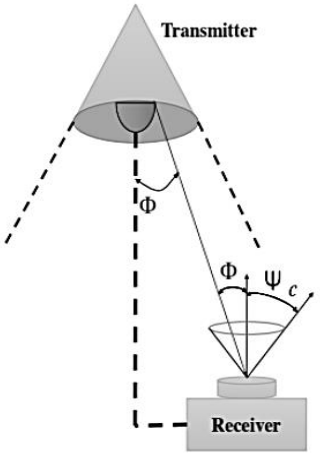

Fig. 1. System model of LOS link.

The brightness of an illuminated surface is measured by illuminance. The angle-dependent luminous intensity is given by [6]

$$I(\phi) = I(0)\cos^m(\phi) \quad (1)$$

The Lambertian radiant order is defined by the semi-angle of half illumination from LEDs, where I is the irradiance angle and m Lambertian radiant order.

$$m = \frac{-\ln 2}{\ln(\cos\psi_C)} \quad (2)$$

The horizontal illuminance E_{hor} is given by:

$$E_{hor} = \frac{I(0)\cos^m(\phi)}{d^2} \times \cos(\Psi) \quad (3)$$

The LOS path's channel DC gain is given in (Figure 1).

$$H(0) = \begin{cases} \frac{(m+1)A}{2\pi d^2}\cos^m(\phi)T_s(\psi)g(\psi)cos(\psi), & 0 \le \psi \le \psi_C \\ 0, & \psi > \psi_C \end{cases} \quad (4)$$

where, A is the physical area of the Photo Detector (PD) detector and ψ is the incident angle. $g(\psi)$, represents the gain of an optical concentrator, and $T_s(\psi)$ denotes the optical filter gain. Ψc , denotes to the field of view at a receiver. The optical concentrator gain is calculated as follows:

$$g(\psi) = \begin{cases} \frac{n^2}{\sin^2(\Psi c)}, & 0 \le \Psi \le \psi_c \\ 0, & 0 \ge \psi_c \end{cases} \quad (5)$$

The optical power received at PD is calculated as follows:

$$P_{re} = H(0) \times P_t \quad (6)$$

where, P_t is transferred power and P_{re} is received power.

2.2 Signal to noise ratio

Light signals will be converted to electrical signals by the photodetector, and the SNR will be shown as [11]:

$$SNR = \frac{i^2}{\sigma^2} \quad (7)$$

where, σ^2 is the total noise variance, i is the output current of the photodiode and are shown as:

$$\sigma^2 = \sigma_{sh}^2 + \sigma_{am}^2 \quad (8)$$

$$i = P\text{re} \times r \quad (9)$$

$$\sigma_{sh}^2 = 2(P\text{re} + P\text{n}) \times q \times r \times B\text{n} \quad (10)$$

$$B\text{n} = I2R\text{b} \quad (11)$$

$$\sigma_{am}^2 = i_{am}^2 B_a \quad (12)$$

where, $\sigma_{am}^2$is the amplifier noise variance, σ_{sh}^2 is the shot-noise variance, r is the photodiode response rate, B_n is the noise bandwidth, P_n is the ambient light's noise power, R_b is data rate, $I^2$is noise bandwidth factor, B_a and i_{am}^2 are the amplifier bandwidth and the noise density, respectively.

2.3 Indoor Configuration

In this research, let us consider the room, which is shaped like a cuboid with non-reflective walls and measures 10 m x 10 m x 3 m. An illumination and communication system is required. LEDs should also function as data transmitters. The lighting infrastructure has a total of 32400 LEDs. The illuminance ranges from 300 to 1500 lx at 32,400. as specified by the International Organization for Standardization (ISO).

Table 1: Parameters and their values

Parameter	Value
Room Measurements	10×10×3 m^3
Total no. of LEDs in the room, N_{LEDr}	32,400
Separation of transmitter and receiver, h	2.15 m
Optical power transmitted per LED, P_{LED}	20 mW
Ambient noise power *P*n	.62 mW
The separation between adjacent LEDs	1 cm
Detector FOV, ψ_{FOV}	70°
Detector's physical area, A	1 cm2
Concentrator gain, $g(\psi)$	6
The filter's transmission coefficient, Ts(ψ)	1

When compared to the width of the room, the separation between successive LEDs on a panel is just 1 cm. As a result, all LEDs are considered to have the same irradiance angle. Later on, the number of panels will be adjusted to produce various configurations of transmitters for research. LED panels are mounted on the plane of the transmitter, which is 25 cm below and parallel to the ceiling of the room. The reception plane, on the other hand, is 60 cm above the room's floor and parallel to it.

For the best performance LED semi-angle $\varphi_{1/2}$ is adjusted from 10° to 90°. The detector's physical area is 1 cm2 and its field of view (FOV) is set to 70 degrees. With a gain of six, the concentrator is used. Because no optical filters are used in this system, the filter's transmission coefficient is set to 1. The system's specifications are summarized in Table 1.

3. EFFECT OF LED SEMI ANGLE

This part explains how to optimise the LED semi-angle ($\varphi_{1/2}$) on the receiver plane for a smooth and high-power distribution pattern. Two parameters determine this: average power received and its change over the receiver's plane. The importance of these two characteristics on the ideal value of semi-angle $\varphi_{1/2}$ is next studied. We use the concept, degree of non-uniformity (D_{nu}), to model and analyse power fluctuations [5]

$$Dnu = \frac{P_{\max}}{P_{min}} \qquad D_{nu} \geq 1 \tag{13}$$

P_{min} is minimum and P_{max} is the maximum valu of optical power obtained over the receiver's plane. D_{nue} should be unity in order to achieve smooth spatial variation.

Consider the following scenario: a room 10x10x3 m^3 with four symmetrically spaced LED panels, as shown in Figure 2.

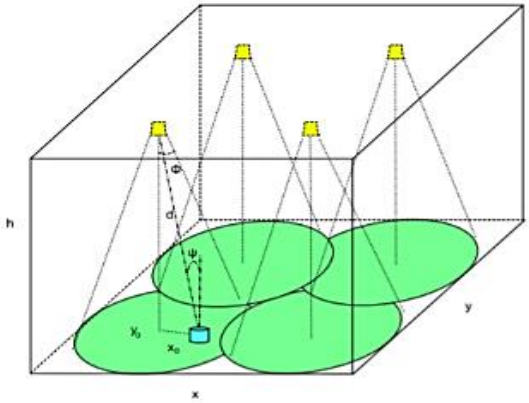

Fig. 2. A room with four LEDs and the footprint of the LEDs [24].

In the room, optical radiation becomes more spread when $\varphi_{1/2}$ of the LED is raised, leading to a decrease in power fluctuations. As the value of $\varphi_{1/2}$ grows, the value of D_{nu} approaches unity, as shown in Figure 3. However, when semi-angle increases, the average power received (P_{avg}) drops since some part of the received power is lost at higher values of $\varphi_{1/2}$. However, raising $\varphi_{1/2}$ lowers the average power received (P_{avg}), because non-reflective walls absorb some transmitted power at higher $\varphi_{1/2}$ values, as seen in Figure 3.

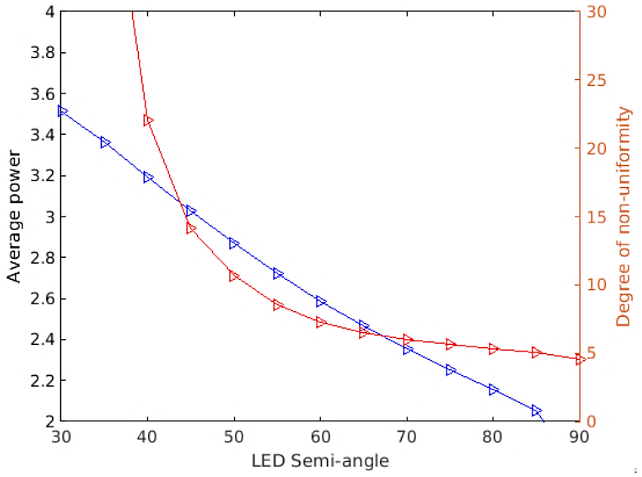

Fig. 3 shows the impact of adjusting the LED $\varphi_{1/2}$ on the average power received Pavg and the degree of non-uniformity (Dnu).

4. OPTIMIZATION OF φ 1/2

P_{avg} and D_{nu} are both important factors in evaluating the output of a VLC connection. As $\varphi_{1/2}$ increases, the power variation (D_{nu}) decreases, resulting in better noise efficiency. However, a high value of $\varphi_{1/2}$ also decreases P_{avg}, which degrades BER performance. This means that when adjusting $\varphi_{1/2}$, there is a trade-off, and would need the use of an optimization method to achieve high P_{avg} and low D_{nu}.
We use an optimisation function

$$F = \frac{(p_{avg})^{\alpha}}{(Dnu)^{\beta}} \tag{14}$$

where, the exponents denote the relative significance of the denominator and numerator parameters, respectively. The value of $\alpha = 0$ or $\beta = 0$ indicates that the relevant parameter is irrelevant.

Both P_{avg} and D_{nu} are $\varphi_{1/2}$ features. As a result, as illustrated by its plot in Figure 8, the optimization function F is similarly a function of the $\varphi_{1/2}$. (Hereafter referred to as the F-plot) Optimization's goal is to locate such value, where F is at its maximum, resulting in a high P_{avg} and a low (above unity) value of D_{nu}. This value of $\varphi_{1/2}$ is defined as the optimal LED semi-angle.

In figure 4 as the $\varphi_{1/2}$ increases, it decreases the Dnu which increases Optimization function, but after the optimum value to $\varphi_{1/2,}$ the function decreases due to loss in received power. This same process is repeated for the various number of panels and studied that how Optimization function varies with every configuration of Leds.

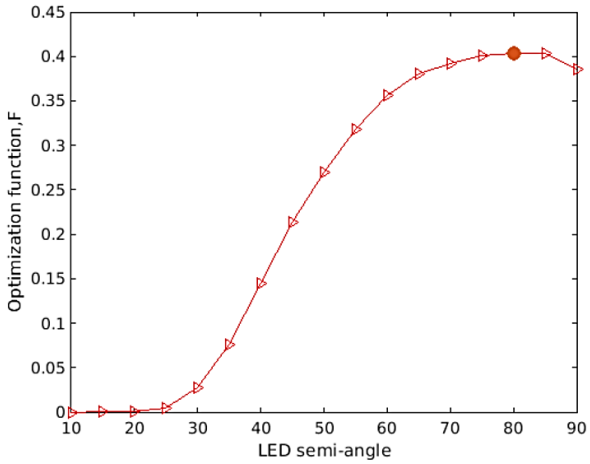

Fig. 4. Semi-angle optimization F-plot with four LED panels uniformly spaced and α = β = 1.

5. EFFECT OF SPATIAL CONFIGURATION OF TRANSMITTER

The effects of altering the spatial layout of LED panels positioned on the transmitter plane are examined first in this section. After that, we look at various transmitter setups and optimise $\varphi_{1/2}$ for each one. The received power is influenced by the position transmitters (x, y, h), and the angle of incidence (which is the same as the irradiance angle at the transmitter).

In addition, if $\varphi > \varphi_{1/2}$, the transmitted power is always less than 50% of its maximum amount, and if $\Psi > \Psi c$, the detector collects no power. The transmitter-to-detector distance, which is determined by the transmitter's setup. This means that the transmitter's position has a big influence on the received power and its fluctuation.

The LEDs are arranged in the uniform configuration of transmitters. The LED panels are arrayed in a square grid in this format, with each panel equidistant from its neighbouring panels. As a result, Np can only have perfect square values. We get diverse configurations by rising the panel count is from Np = 4 (2x2) to Np = 81 (9x9).

However, D_{nu} drops dramatically as Np rises (Figure 5). As a result, the F-plots continue to shift upwards, as seen in Figure 6, where phi (represented by little circles) is decreasing. With the maximum amount of Np, Np = 81, the maximum F-plot is obtained, and hence it can be declared the best uniform transmitter configuration. In figure 6 highest value of the plot is when the Np= 81(9x9). Figure 5 depicts the smallest value of D_{nu} is also at Np=81. Hence the optimum LED configuration can be considered to 81(9x9) with the $\varphi_{1/2}$ =20.

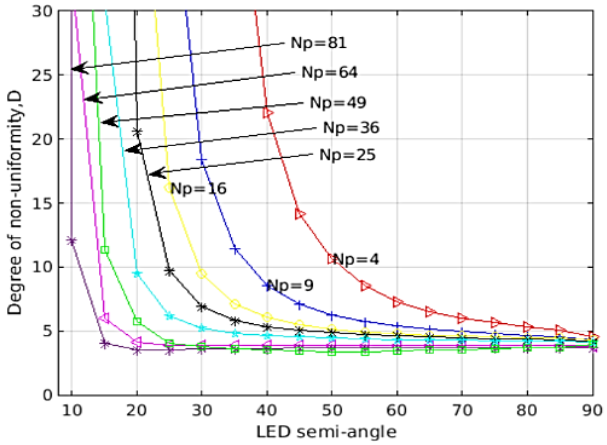

Fig. 5. Effect of LED's semi-angle and panel count on the degree of non-uniformity, Dnu, in a uniform setup.

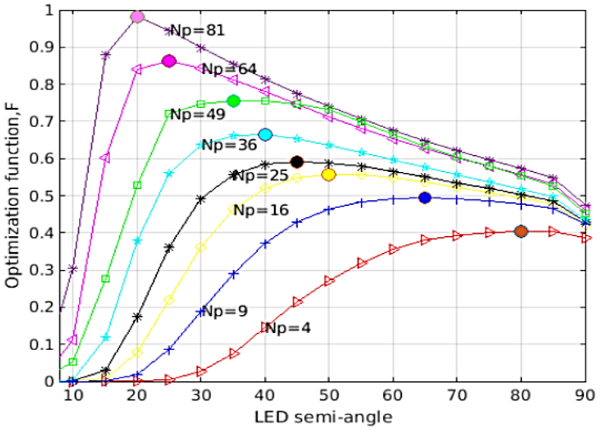

Fig. 6. Function plots with Np = 4 (2x2) to 81 (9x9) optimised for various uniform setups. On each plot, the little circles show how $\varphi_{1/2}$ varies as Np varies.

6. DIFFERENTIAL OPTICAL RECEIVER

In their most basic form, optical laser receivers consist of a single photodetector. Sunlight, in the absence of any filtration, produces a powerful DC current. A laser signal that has been transmitted over a long distance will be overpowered by strong sunlight. The photocurrent produced by all ambient light, including sunshine, is unrelated to the laser signals. As shown in Figure 7, two photoreceivers are crossed-coupled. As a result, the total output power is either 0 or near zero (Figure 7). The laser signal is overwhelmingly dominating after all other signals have been canceled, and it is demodulated and decoded via code correlation [10]. The shot-noise altered as a result.

$$\sigma_{sh}^2 = 2(P_{re}) \times q \times r \times B_n \quad (15)$$

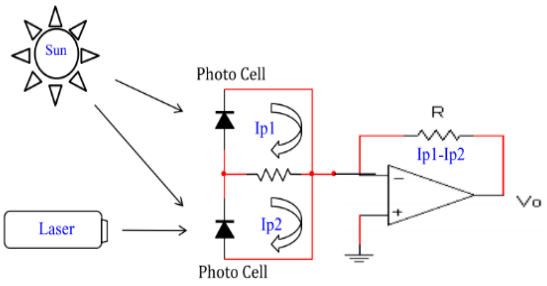

Fig. 7. The sunlight is suppressed using a differential optical receiver. Ambient light and an optical signal produce photocurrents Ip1 and Ip2.

7. OPTICAL POWER DISTRIBUTION SIMULATION

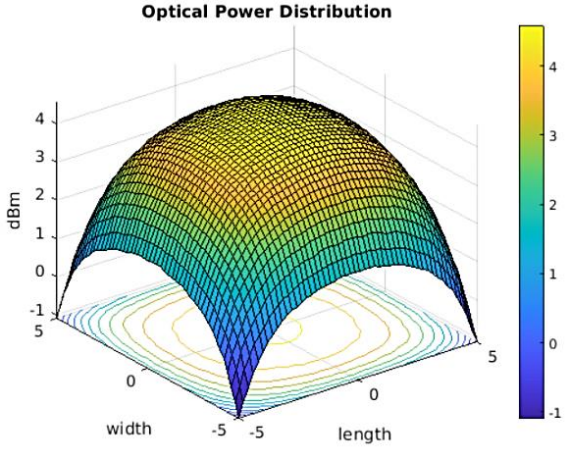

Fig 8. Optical power distribution $\varphi_{1/2}$=80(Np=81).

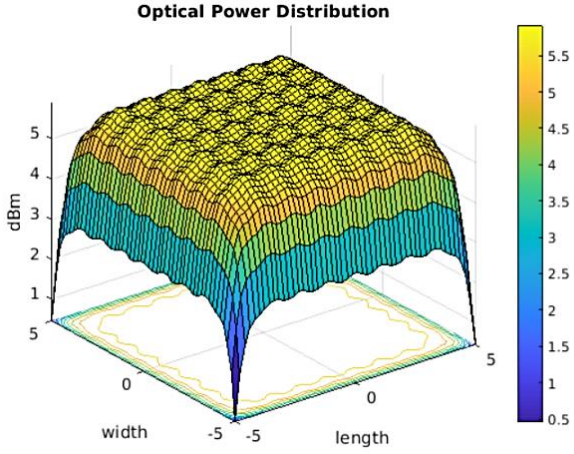

Fig. 9. Optical power distribution $\varphi_{1/2}$=20 (Np=81).

Figure 8 shows optical power distribution at $\varphi_{1/2}$ =80°. At semi-angle $\varphi_{1/2}$ =80° with a maximum power of 4.2 dBm, the distribution of optical power is approximately evenly scattered around the center. However, with this half-angle ($\varphi_{1/2}$) we cannot achieve uniform power distribution and because of higher values of ϕ1/2, non-reflective walls absorb some of the transmitted power.

Therefore, we modeled the distribution of optical power at the optimized semi-angle of 20° (figure 9). The results of this simulation, as shown in Figure 9, reveal that a maximum power of 5.5 dBm. The received power is higher in $\varphi_{1/2}$ =20° with this half-angle, however, we can attain a uniform power distribution. With the higher received power, we can achieve a uniform power distribution in this half-angle.

8. SNR SIMULATION

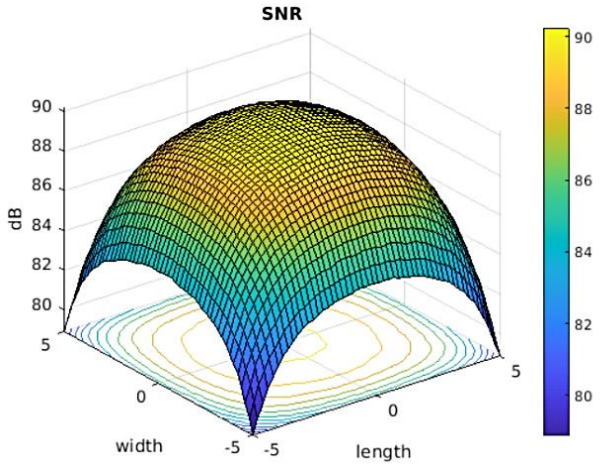

Fig. 10. SNR distribution at $\varphi_{1/2}$=80 (Np=81)

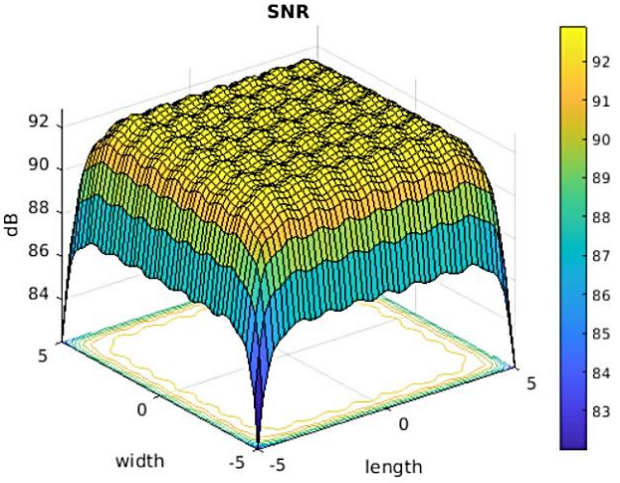

Fig 11. SNR distribution at $\varphi_{1/2}$=20(Np=81).

Figure 10 depicts the stimulation results of 81(9x9) panels in a 10x10x3 m^3 room with 0.62 dB ambient noise. The simulation was conducted at semi-angle 80, with received SNR levels ranging from 90 to 79 decibels.

The simulation results of the proposed model are displayed in Figure 11 is after using a differential optical receiver and an Optimized semi-angle at half power of 20° instead of 80°. It shows an output SNR ranging from 82 to

92.9 dB, as well as noise reduction. Instead of 90 dB, the following model achieves a maximum SNR of 92.9 dB.

9. CONCLUSION

This research looked into the impact of LED semi-angle (φ1/2) and configurations of transmitters on the distribution pattern of power received in the indoor VLC link. Power variances (modeled by the non-uniformity degree, D_{nu}) diminish as $\varphi_{1/2}$ increases, but average received power (P_{avg}) also decreases. For a uniform four-panel arrangement, we used optimization methodology for φ1/2 and found that its optimal value is φ1/2= 80°.

Finally, the authors have investigated the uniform designs with varied panel counts, NP, using the same optimization approach (with $\alpha = \beta = 1$). The uniform configuration with NP = 81 (φ1/2 = 20°) was found to be the best. The given optimization technique is a potential methodology for assuring adequate illumination and obtaining the best value of φ1/2 for every setup of the transmitter in an indoor VLC link. It's also possible to utilise it to analyze several transmitter setups for the same value of φ1/2. Figure 8 and Figure 9 are shown the received power of 81 (9x9) led panels configuration at 80 and 20 semi-angles at half power respectively. At the 20 the power distribution is more uniform and higher received power. Figure 10 and Figure 11 are shown the SNR of 81(9x9) led panels configuration at 80 and 20 semi-angles at half power after respectively. The improved model shows an output SNR ranging from 82 to 92.9 dB, as well as noise reduction. Instead of 90 dB, the following model achieves a maximum SNR of 92.9 dB. In terms of received power, the overall coverage area of the room was enhanced as compared to the four Np setup, according to the results.

ACKNOWLEDGMENT

The Authors are profoundly thankful to the Department of Electronics Engineering, the Indian Institute of Technology (Banaras Hindu University), Varanasi (Uttar Pradesh) India for providing the resources and facilities required to accomplish this research work. This innovative research work is dedicated to loving memories of the first author's grandmother parinivutta Subhadra Devi Verma Ji, who passed away on May 28, 2009 and Parinivutta Yashoda Devi Verma Ji who passed away on August 23, 2021.

REFERENCES

[1] Z. Ghassemlooy, S. Arnon, M. Uysal, Z. Xu and J. Cheng, "Emerging optical wireless communications – advances and challenges," IEEE Journal on Selected Areas in Communications, vol. 33, no. 9, pp. 1738- 1749, Sept. 2015.

[2] M. D. Soltani, X. Wu, M. Safari and H. Haas, "Bidirectional user throughput maximization based on feedback reduction in LiFi networks," IEEE Transactions on Communications, vol. 66, no. 7, pp. 3172-3186, July 2018.

[3] P. Ge, X. Liang, J. Wang, C. Zhao, X. Gao and Z. Ding, "Optical filter designs for multi-color visible light communication," IEEE Transactions on Communications, vol. 67, no. 3, pp. 2173-2187, March 2019.

[4] D. Karunatilaka, F. Zafar, V. Kalavally, and R. Parthiban, "LED based indoor visible light communications: state of the art," IEEE Communications Surveys & Tutorials, vol. 17, no. 3, pp. 1649-1678, 2015.

[5] K. Saxena, R. Raj and A. Dixit, "A novel optimization approach for transmitter semi-angle and multiple transmitter configurations in indoor visible light communication links," in 2018 9th IEEE International Conference on Computing, Communication and Networking Technologies (ICCCNT), Bangalore, 2018, pp. 1-7

[6] T. Komine and M. Nakagawa, "Fundamental analysis for visible-light communication system using LED lights," IEEE Trans. Consum. Electron., vol. 50, no. 1, pp. 100– 107, Feb. 2004.

[7] H. Chun, C. J. Chiang, and D. C. O'Brien, "Visible light communication using OLEDs: Illumination and channel modeling," in 2012 International Workshop on Optical Wireless Communications (IWOW), Pisa, 2012, pp. 1-3.

[8] H. Q. Nguyen, J.-H. Choi, M. Kang, Z. Ghassemlooy, D. H. Kim, S.-K. Lim, T.-G. Kang, and C. G. Lee, "A MATLAB-based simulation program for indoor visible light communication system," in 2010 7th International Symposium on Communication Systems, Networks & Digital Signal Processing (CSNDSP 2010), Newcastle upon Tyne, 2010, pp. 537-541.

[9] T. Komine and M. Nakagawa, "Fundamental analysis for visible-light communication system using LED lights," in IEEE Transactions on Consumer Electronics, vol. 50, no. 1, pp. 100-107, Feb 2004.

[10] S.-Faruque, S.- Faruque, and W.-Semke, "- Orthogonal on–off keying for free-space laser communications with ambient light cancellation," - *Opt. Eng.*, vol. 52,no. 9, p. 096113, 2017.

[11] H. Lu, Z. Su, and B. Yuan, "SNR and Optical Power Distribution in an Indoor Visible Light Communication System," pp. 1063–1067, 2014.

[12] Sanjeev Mani Yadav, and Amritanshu Pandey, Highly Efficient and Broadband Hybrid Photodetector Based on 2D Layered Graphene / CTS Quantum Dots, IEEE Trans Electron Device, 66, 8, 3417-3424 2019

[13] Y. Kumar, H. Kumar, B. Mukherjee, G. Rawat, C. Kumar, B. N. Pal and **S.** Jit, "Visible-blind Au/ZnO Quantum Dots based Highly Sensitive and Spectrum Selective Schottky Photodiode," *IEEE Trans. Electron Devices*, Vol. 64, No. 7, pp. 2874 - 2880, July 2017.

[14] Peng-Cheng Song, Zi-Yang Wu, Xiao-Dong An, Jiao Wang, "Energy Efficiency Analysis of Light-Emitting Diodes With High Modulation Bandwidth" *IEEE Trans. Electron Devices*, Vol. 42, No. 7, pp. 1025 - 1028, July 2021.

[15] Agon Memedi, Falko Dressler, **"**Vehicular Visible Light Communications" *IEEE Communications Surveys & Tutorials*, vol. 23, no. 1, pp. 161 - 181, 2021.